Research Square

Preprints are preliminary reports that have not undergone peer review.
They should not be considered conclusive, used to inform clinical practice,
or referenced by the media as validated information.

High Concordance in Molecular Profiles Between Primary Tumors and Matched Lymph Node Metastases in Differentiated Thyroid Carcinoma: Implications for Clinical Sample Selection

Yijin Pan
Chinese Academy of Medical Sciences & Peking Union Medical College
Yuqing Sun
Beijing Tsinghua Chang Gung Hospital
Cong Shi
Chinese Academy of Medical Sciences & Peking Union Medical College
Ruochen Li
Chinese Academy of Medical Sciences & Peking Union Medical College
Liming Xu
Amoy Diagnostics Co., Ltd
Changbin Zhu
Amoy Diagnostics Co., Ltd
Yansong Lin
linys@pumch.cn

Chinese Academy of Medical Sciences & Peking Union Medical College

Article

Keywords: differentiated thyroid carcinoma, genetic alteration, genetic testing, clinical decision-making, tumor heterogeneity

Posted Date: June 24th, 2026

DOI: https://doi.org/10.21203/rs.3.rs-9922971/v1

License: This work is licensed under a Creative Commons Attribution 4.0 International License. Read Full License

Additional Declarations: No competing interests reported.

Version of Record: A version of this preprint was published at Scientific Reports on October 20th, 2026. See the published version at https://doi.org/10.1038/s41598-026-73502-x.

Abstract

Genetic testing guides personalized management of differentiated thyroid carcinoma (DTC). However, tumor heterogeneity, including spatial and temporal heterogeneity, has created an unresolved clinical problem. It remains unclear whether molecular profile of the primary tumor (PT) can reliably reflect the genetic characteristics of paired lymph node metastases (LNM) to reduce redundant testing costs. We analyzed 63 paired primary tumor-lymph node metastasis (PT-LNM) samples from 55 Chinese patients with DTC using a 10-gene real-time PCR assay to evaluate spatial heterogeneity. To assess the impact of temporal heterogeneity, we further stratified pairs into synchronous groups (≤ 6 months between PT resection and LNM detection, n = 41) and asynchronous groups (> 6 months interval, n = 22). The overall molecular concordance rate between PT and LNM was 88.9%. Concordance rates for core driver alterations ranged from 92.1% to 100%, with Cohen's Kappa values of 0.79–1.00. Specifically, *BRAF* V600E mutation showed 92.1% concordance, *TERT* promoter mutation showed 98.4% concordance, and *RET*/*NTRK3* fusions showed 98.4%-100% concordance. No statistically significant differences were detected between PT and LNM in overall or subgroup analyses (all P > 0.05). Our findings indicate high and time-independent molecular concordance between PT and LNM in Chinese DTC patients. This supports the clinical utility of PT-only genetic testing to guide LNM management.

1. Introduction

Thyroid cancer is the most common endocrine malignancy. In 2022, 466,100 new cases were reported in China, ranking third among all cancer incidences [1]. Differentiated thyroid carcinoma (DTC), mainly including papillary thyroid carcinoma (PTC) and follicular thyroid carcinoma (FTC), accounts for more than 90% of all thyroid cancer cases, and approximately 30% of DTC patients develop lymph node metastasis (LNM) at diagnosis or during follow-up [2–7]. LNM development is closely related to driver mutations such as *BRAF* V600E and *TERT* promoter (*TERT*p) mutations, which not only indicate aggressive tumor behavior but also represent actionable targets for *BRAF/MEK* inhibitor therapy. Therefore, genetic testing is critical for recurrence risk stratification and personalized treatment selection for DTC patients with LNM [8, 9].

Despite the established clinical value of genetic testing, tumor heterogeneity poses a longstanding unresolved clinical dilemma: to date, there is insufficient high-quality evidence to confirm whether molecular testing of primary tumor (PT) tissue alone can reliably reflect the actionable molecular profile of matched LNM lesions. Tumor heterogeneity encompasses genetic, phenotypic, and functional diversity among cancer cell populations, and is broadly categorized into two dimensions: spatial heterogeneity (genetic differences between anatomically distinct lesions at the same time point) and temporal heterogeneity (dynamic changes in tumor clonal architecture during disease progression) [10–12]. According to the clonal evolution theory, tumors are composed of multiple genetically distinct subclones, and only subclones with high invasive potential are thought to successfully metastasize to regional lymph nodes. This biological selection process could theoretically result in molecular discordance between PT and matched LNM [13–15]. Testing PT tissue alone may therefore miss actionable alterations present exclusively in LNM, potentially leading to suboptimal treatment decisions. Conversely, routine simultaneous testing of both PT and LNM would increase patient financial burden and healthcare resource utilization due to additional sampling and testing costs, especially in resource-limited settings.

To address this clinical dilemma, it is necessary to systematically evaluate the genetic concordance between PT and matched LNM in DTC. However, previous studies on this topic are very limited, and most of which are conducted in Western populations, with limited applicability to Chinese patients. Furthermore, few prior studies have explored the impact of LNM occurrence timing on molecular concordance, leaving the potential effect of temporal heterogeneity largely uncharacterized [16–21].

To fill these gaps, this prospective cohort study included 63 pathologically confirmed primary tumor-lymph node metastasis (PT-LNM) pairs from 55 Chinese DTC patients. We performed targeted molecular profiling of paired samples using a clinically validated 10-gene real-time PCR panel, and stratified pairs into synchronous group (interval ≤ 6 months between PT resection and LNM detection, n = 41) and asynchronous group (interval > 6 months, n = 22) to evaluate both spatial and temporal heterogeneity of driver alterations. The findings of this study are expected to provide evidence-based guidance for genetic testing sample selection in routine clinical practice.

2. Materials and Methods

This prospective cohort study was approved by the Ethics Committee of Peking Union Medical College Hospital (approval number: K6879) and conducted in full compliance with the Declaration of Helsinki. Written informed consent was obtained from all participants. For minor participants, written informed consent was obtained from their legal guardians. **2.1 Study Participants**

We initially recruited 134 thyroid cancer patients receiving long-term follow-up at the Nuclear Medicine Department of Peking Union Medical College Hospital between June 2024 and December 2025.

Inclusion criteria: 1) Pathologically confirmed DTC after total or subtotal thyroidectomy; 2) Pathologically confirmed LNM, with both PT and matched LNM tissue samples available for genetic testing; 3) Signed informed consent.

Exclusion criteria: 1) Concurrent or history of other active malignant tumors within 5 years; 2) Incomplete clinical data insufficient for analysis; 3) Failed genetic testing due to tissue degeneration, insufficient tumor content, or ambiguous testing sites.

After screening, 63 PT-LNM pairs from 55 eligible patients were included in the final analysis. Seven patients contributed multiple PT-LNM pairs (1 patient with 3 pairs, 6 patients with 2 pairs each), resulting in a discrepancy between the number of pairs (63) and patients (55) (Figure 1).

2.2 Clinicopathological Data Collection

The following data were extracted from electronic medical records:

Demographic characteristics: Age at diagnosis, gender, follow-up duration (defined as the interval from thyroidectomy to the last visit).

Clinicopathological characteristics: Pathological subtype (classified according to the 5th edition WHO Tumor Classification [2]), recurrence risk stratification (stratified into intermediate/high risk per the 2025 ATA Guidelines [4]), number of thyroid surgeries, maximum PT diameter, T stage, N stage, distant metastasis status, and overall stage (per the 9th edition AJCC guidelines).

2.3 Molecular testing

DNA and RNA extraction. Formalin-fixed paraffin-embedded (FFPE) tissue, fresh-frozen tissue, or fine-needle aspiration (FNA) samples were collected from PTs and matched LNMs. Genomic DNA and total RNA were extracted using commercially available kits according to the manufacturers' protocols.

Somatic mutation detection. Qualitative detection of somatic mutations in *BRAF* V600E, *NRAS*, *HRAS*, *KRAS*, *TERT*p, and *PIK3CA* was performed by ADx-ARMS® (Amplification Refractory Mutation System) real-time PCR on the SLAN-96S real-time PCR system (or QuantStudio 5, as applicable) using the AmoyDx® Thyroid Cancer PCR Panel (Amoy Diagnostics, Xiamen, China). The assay discriminates mutant alleles from wild-type sequences via allele-specific primers and fluorescent probes (FAM/ROX channels), with an internal control gene co-amplified in each reaction to verify sample quality and PCR efficiency.

Gene fusion detection. *RET*, *PPARG*, *NTRK1*, and *NTRK3* gene fusions were detected by one-step RT-PCR using primers and probes spanning the fusion junctions. The assay was performed on the same real-time PCR platform as above. Positive fusion calls were determined by the emission of FAM or ROX fluorescence signals, with each reaction containing an internal reference to assess RNA integrity and transcription efficiency.

Quality control and interpretation. Samples were considered adequate only when the internal control yielded a valid cycle threshold (Ct) value. A sample was defined as mutation-positive or fusion-positive when the target fluorescent signal exceeded the preset threshold and showed a characteristic amplification curve, as interpreted by the accompanying analysis software. Samples failing internal control amplification were excluded from further analysis.

Concordance analysis. The molecular profiles of PTs and matched LNMs were compared on a per-alteration basis. Concordance was defined as the detection of identical actionable alterations in both specimens; discordance was defined as the presence of an alteration in one specimen but not the other.

2.4 Statistical Analysis

Continuous variables were tested for normality using the Shapiro-Wilk test: normally distributed data were compared using the independent samples t-test and presented as mean ± standard deviation; non-normally distributed data were compared using the Mann-Whitney U test and presented as median (interquartile range, P25-P75). Categorical variables were compared using the chi-square test or Fisher's exact test. PT-LNM pairs were stratified into synchronous group (interval between PT and LNM occurrence ≤6 months, n=41) and asynchronous group (interval >6 months, n=22) to evaluate the impact of temporal heterogeneity on concordance. Cohen's Kappa coefficient was used to quantify the level of concordance, with Kappa ≥0.75 indicating excellent agreement. All statistical analyses were performed using R Studio (version 4.1.0), with a two-sided $P<0.05$ considered statistically significant.

3. Results

3.1 Clinicopathological characteristics of included patients

The 55 included patients had a median follow-up duration of 27.7 (11.9, 59.3) months, with a male-to-female ratio of 1:2.1. Pathological subtypes included PTC (96.4%, 53/55) and FTC (3.6%, 2/55). All patients underwent total or near-total thyroidectomy, and 43.6% (24/55) had undergone ≥2 thyroid surgeries. The median maximum PT diameter of the patients was 2.0 cm (1.3, 3.7). 38.2% (21/55) of the patients were diagnosed with T3a-T4b stage disease. 98.2% (51/55) of the patients had N1b stage disease. 80.0% (44/55) of the patients had distant metastasis, among whom 95.5% had lung-only metastasis. 87.3% (48/55) of the patients were classified as high recurrence risk. 72.7% (40/55) of the patients were at overall stage II disease (Table 1).

3.2 Concordance of genotypes between PTs and matched LNMs in overall analysis

Among all 63 PT-LNM pairs, the genetic alteration detection rates were 78.8% (50/63) in PTs and 71.4% (45/63) in matched LNMs. The overall concordance rate of genetic testing results between PTs and LNMs was 88.9% (56/63). Among all the gene alterations detected in this study, the alterations identified include *BRAF* V600E mutation, *TERT*p mutation, *NTRK3* fusion, and *RET* fusion. The frequency of *BRAF* V600E mutation was 46.0% (29/63) in PTs and 38.1% (24/63) in LNMs, with a concordance rate of 92.1% (58/63) (Kappa coefficient: 0.83). *TERT*p mutation was detected in 3.2% (2/63) of PTs and 4.8% (3/63) of LNMs, with a concordance rate of 98.4% (62/63) (Kappa coefficient: 0.79). *NTRK3* fusion was found in 4.8% (3/63) of PTs and 3.2% (2/63) of LNMs, with a concordance rate of 98.4% (62/63) (Kappa coefficient: 0.79). *RET* fusion was detected in 30.2% (19/63) of PTs and 30.2% (19/63) of LNMs, with a 100.0% concordance rate (63/63) (Kappa coefficient: 1.00) (Table 2).

Discordant molecular profiles were observed in 11.1% (7/63) of PT-LNM pairs, including 5 cases with *BRAF* V600E mutation detected only in PT but not in matched LNM, 1 case with *BRAF* V600E mutation combined with *NTRK3* fusion in PT but only *BRAF* V600E mutation in LNM, and 1 case with *BRAF* V600E mutation in both PT and LNM plus additional *TERT*p mutation detected only in LNM (Figure 2).

3.3 Concordance of genotypes between PTs and matched LNMs in synchronous group

Subgroup analysis showed that in the synchronous group, the genetic alteration detection rates were 75.6% (31/41) in PTs and 65.9% (27/41) in LNMs, with a concordance rate of 87.8% (36/41). The frequency of *BRAF* V600E mutation was 39.0% (16/41) in PTs and 29.3% (12/41) in LNMs, with a concordance rate of 90.2% (37/41) (Kappa coefficient: 0.79). No *TERT*p mutation was detected in either PTs or LNMs in the synchronous group, resulting in a 100.0% concordance rate (41/41) (Kappa coefficient: 1.00). *NTRK3* fusion was found in 4.9% (2/41) of PTs and 2.4% (1/41) of LNMs, with a concordance rate of 97.6% (40/41) (Kappa coefficient: 0.66). *RET* fusion was detected in 34.1% (14/41) of PTs and 34.1% (14/41) of LNMs, with a 100.0% concordance rate (41/41) (Kappa coefficient: 1.00) (Table 3).

Discordant genetic profiles were observed in 12.2% (5/41) of pairs in the synchronous group, including 4 cases with *BRAF* V600E mutation only in PT, and 1 case with *BRAF* V600E mutation combined with *NTRK3* fusion in PT but only *BRAF* V600E mutation in LNM.

3.4 Concordance of genotypes between PTs and matched LNMs in asynchronous group

In the asynchronous group, the genetic alteration detection rates were 86.4% (19/22) in PTs and 81.8% (18/22) in LNMs, with a concordance rate of 90.9% (20/22). The frequency of *BRAF* V600E mutation was 59.1% (13/22) in PTs and 54.5% (12/22) in LNMs, with a concordance rate of 95.5% (21/22) (Kappa coefficient: 0.91). *TERT*p mutation was detected in 9.1% (2/22) of PTs and 13.6% (3/22) of LNMs, with a concordance rate of 95.5% (21/22) (Kappa coefficient: 0.78). *NTRK3* fusion was found in 4.5% (1/22) of PTs and 4.5% (1/22) of LNMs, with a 100.0% concordance rate (22/22) (Kappa coefficient: 1.00). *RET* fusion was detected in 22.7% (5/22) of PTs and 22.7% (5/22) of LNMs, with a 100.0% concordance rate (22/22) (Kappa coefficient: 1.00) (Table 4).

Discordant genetic profiles were observed in 9.1% (2/22) of pairs in the asynchronous group, including 1 case with *BRAF* V600E mutation only in PT, and 1 case with *BRAF* V600E mutation in PT but *BRAF* V600E mutation combined with *TERT*p mutation in LNM.

3.5 Comparison of genotypes between PTs and matched LNMs

Statistical analysis revealed no significant differences in the distribution of genetic alterations between PTs and matched LNMs across all 63 PT-LNM pairs (all $P > 0.05$) (Table 5). Subgroup analysis further confirmed that there were no statistically significant differences in genetic profiles between PTs and matched LNMs in either the synchronous group or the asynchronous group ($P > 0.05$) (Figure 3).

4. Discussion

This study was designed to address the common clinical dilemma of genetic testing sample selection for DTC patients with confirmed LNM, by systematically evaluating the molecular profile concordance between paired primary tumor (PT) and LNM samples, with a specific focus on the impact of LNM occurrence timing on concordance. Our findings reveal a high overall molecular concordance rate of 88.9% between PT and matched LNM in this Chinese DTC cohort, which suggests that molecular testing of PT tissue alone may effectively guide clinical management of LNM in most cases, potentially reducing unnecessary testing burden for patients. It is noteworthy that our cohort was enriched for patients with advanced TN stages, high recurrence risk, and distant metastasis, populations for whom genetic testing carries particularly high clinical decision-making value compared to low-risk patient groups.

To our knowledge, this work has three distinct methodological and clinical strengths that contribute to the existing literature. First, it is one of the most recent studies focusing on an East Asian cohort of DTC patients with pathologically confirmed LNM, addressing a critical gap in region-specific evidence given the distinct epidemiological and genetic profiles of DTC in Chinese populations. Second, it is among the first studies to systematically evaluate the impact of temporal heterogeneity on molecular concordance, providing preliminary evidence that PT testing results may remain valid even for delayed LNM occurring years after initial PT resection. Third, it employs a widely accessible, low-cost 10-gene real-time PCR panel that is already implemented in routine clinical practice across China, making study findings potentially directly translatable to real-world clinical settings. The key findings of our study include the 88.9% overall molecular concordance rate, with core driver alterations showing concordance rates of 92.1% for *BRAF* V600E, 98.4% for *TERT*p mutation, 98.4% for *NTRK3* fusion, and 100% for *RET* fusion.

The 88.9% overall concordance rate observed in our study is consistent with the 85% to 92% concordance rate reported in previous Western cohorts [19, 20]. Melo et al. [19] analyzed 437 tissue samples from 204 thyroid cancer patients. They found that *BRAF* mutation rates were 44.6% in primary PTC and 41.7% in matched LNM, with significant genotypic consistency. Fakhruddin et al. [20] similarly confirmed high conservation of *BRAF* mutations between primary and metastatic lesions in 253 PTC patients. The Kappa value was 0.77, with $P < 0.0001$. This finding indicates that *BRAF* mutation is an early driver event in thyroid tumorigenesis. Notably, our study is one of the first to report this high concordance feature in a Chinese DTC cohort with LNM. It extends the generalizability of previous findings to East Asian populations. DTC incidence is rising rapidly in this region, and driver alteration profiles differ from Western populations. From the clonal evolution perspective, this high consistency can be well explained by the linear metastasis model. Most LNM originate from the dominant clone of PT. This clone retains core driver genetic alterations during the metastatic process. Thus the molecular profile of PT is preserved in metastatic lesions [11–13]. These dominant clones gain growth and invasion advantages through early driver events, and become the main population colonizing lymph nodes. The clinical implication of this high concordance is straightforward. Genetic testing of PT alone could effectively reflect the actionable molecular characteristics of matched LNM. Routine repeated testing of LNM is not necessary for clinical decision-making. This strategy can reduce unnecessary tissue sampling, testing costs and sample loss for patients. It is particularly valuable for primary healthcare settings with limited medical resources.

In our cohort, the concordance rate of *BRAF* V600E mutation between PT and matched LNM was 92.1%, with a Kappa value of 0.83, which is comparable to the 85%–94% concordance rate reported in previous multi-ethnic studies [19, 20]. *BRAF* V600E is recognized as an early driver event in DTC, which constitutively activates the MAPK signaling pathway, promotes cell proliferation and invasion, and is closely associated with LNM and high recurrence risk [20, 21]. The high conservation of this mutation between primary and metastatic lesions suggests that *BRAF* V600E status detected in PT may reliably guide *BRAF* inhibitor therapy for both primary and metastatic lesions. For patients with *BRAF* V600E-positive PT, even if LNM tissue is unavailable, BRAF-targeted therapy could still be considered for advanced or radioactive iodine-refractory disease, potentially avoiding the need for additional invasive biopsy of metastatic lesions. Notably, *RET* fusion showed a 100% concordance rate between PT and matched LNM in our cohort, with a Kappa value of 1.00, indicating almost perfect agreement. *RET* fusion is another well-characterized early driver event of DTC, which occurs via non-homologous end joining of double-strand DNA breaks in the early stage of tumorigenesis, and continuously activates tyrosine kinase signaling to promote cell migration and survival [22, 23]. The perfect consistency of *RET* fusion observed in our cohort suggests that this alteration is acquired in the very early stage of tumorigenesis, exists in almost all tumor cells of the dominant clone, and remains stable during metastasis. This finding provides preliminary strong evidence for *RET* inhibitor therapy based solely on PT testing. For *RET* fusion-positive DTC patients with LNM, targeted therapy could potentially be initiated without additional testing of metastatic lesions, which is of particular value for unresectable LNM cases where tissue sampling is difficult or associated with high complication risk. The concordance rates of *TERT*p mutation and NTRK3 fusion were both 98.4%, with a Kappa value of 0.79, indicating substantial agreement between PT and LNM. *TERT*p mutation is a well-established late event in DTC progression, associated with dedifferentiation and iodine refractoriness [14, 24–26]. The high concordance of this mutation suggests that *TERT*p status in PT may reliably predict its presence in LNM, which could help identify patients who require more aggressive treatment and closer follow-up.

Previous studies on PT-LNM molecular concordance mostly focused on spatial heterogeneity, while the impact of temporal heterogeneity, such as the time interval between PT and LNM occurrence, has been rarely explored. Our study innovatively introduced LNM occurrence time as a key variable, and divided PT-LNM pairs into synchronous group (interval ≤ 6 months, $n = 41$) and asynchronous group (interval > 6 months, $n = 22$) for subgroup analysis. The results showed that the high concordance remained stable regardless of the time interval. The concordance rate was 87.8% in the synchronous group and 90.9% in the asynchronous group. This finding has important clinical implications that the molecular profile of PT is applicable not only to synchronous LNM detected at initial surgery, but also to asynchronous LNM occurring months or even years after initial treatment. This further supports the clinical recommendation that PT genetic testing results could guide the treatment of metastatic lesions even when LNM occurs during long-term follow-up.

Despite the overall high concordance, 11.1% (7/63) of PT-LNM pairs showed discordant molecular profiles in our cohort. Among these discordant pairs, 85.7% (6/7) had more genetic alterations detected in PT than in matched LNM, including 5 cases with *BRAF* V600E mutation only present in PT, and 1 case with concurrent *BRAF* V600E mutation and NTRK3 fusion in PT but only *BRAF* V600E mutation in LNM. This phenomenon could be explained by the branched evolution model: PT contains multiple subclones with different genotypes, and only subclones with high invasive and metastatic ability are thought to successfully colonize lymph nodes [11–13]. The subclones carrying alterations only present in PT may lack metastatic potential, thus not participating in LNM formation. Additionally, metastatic clones may lose specific alterations during adaptation to the lymph node microenvironment, such as downregulating immunogenic mutations to evade immune surveillance, leading to undetectable alteration levels below the testing threshold [27–28]. The lower mutational burden observed in lymph node metastases compared with primary tumors in our discordant pairs is also consistent with the evolutionary bottleneck theory of metastasis, which states that metastatic colonization is a stringent selective process that reduces clonal diversity in metastatic lesions relative to the primary tumor. Notably, *BRAF* V600E had the lowest concordance rate among all tested driver alterations in our cohort. This finding may be attributed to two potential reasons: first, *BRAF* V600E may exist in subclones with lower metastatic potential in some cases, which are not selected during the metastatic process; second, intra-tumoral heterogeneity of PT may lead to sampling bias, where the tested PT tissue contains BRAF-positive subclones while the metastatic clone originates from a BRAF-negative region of the PT. Only one case in our cohort showed additional *TERT*p mutation in LNM but not in matched PT, which belonged to the asynchronous group with a 9.5-year interval between PT resection and LNM detection. This indicates that new driver alterations may accumulate in metastatic lesions during long-term disease progression. The co-occurrence of *BRAF* V600E and *TERT*p mutation is a well-established high-risk

prognostic factor for DTC, which significantly increases the risk of disease progression and poor prognosis [29–30]. For such patients, even if *TERT*p mutation is not detected in PT, dynamic monitoring of disease progression is still recommended, and re-biopsy of new metastatic lesions may be considered when disease progresses rapidly to adjust treatment strategies. It should be emphasized that even in this discordant case, the *BRAF* V600E status was still consistent between PT and LNM, suggesting that the core driver alteration guiding targeted therapy remains stable, and PT testing is still sufficient for first-line treatment decision-making.This study has two main limitations: first, we only included PT and LNM samples, and did not analyze distant metastatic lesions. Given that distant metastases may acquire more additional alterations during longer evolutionary processes, further studies are needed to explore the molecular concordance between distant metastases and primary lesions. Second, this is a single-center study with a relatively small sample size, especially for the asynchronous subgroup. Multicenter, large-scale prospective cohorts are needed to further validate the generalizability of our findings.

5. Conclusion

This study is among the first to systematically analyze the concordance in molecular profiles between PT and matched LNM in a Chinese cohort of DTC patients with pathologically confirmed LNM. We innovatively incorporated the time interval between PT resection and LNM detection to investigate the impact of temporal heterogeneity on molecular concordance. Our results demonstrate a high degree of concordance in core driver molecular profiles between PT and LNM, and this concordance appears not to be affected by the timing of LNM occurrence. Most discordant cases showed more genetic alterations in PT than in LNM, which is consistent with the branched evolution model of tumor metastasis. In clinical practice, molecular testing of PT specimens alone may capture the vast majority of actionable alterations present in LNM, providing reliable guidance for the clinical management of metastatic disease in most cases. This strategy could potentially reduce patient economic burden, optimize pathological resource utilization, and improve the efficiency of genetic testing implementation in routine clinical care. Further large-scale multicenter studies are warranted to confirm these findings and establish evidence-based guidelines for genetic testing sample selection in DTC patients with LNM.

Declarations

Funding

This study is supported by National High Level Hospital Clinical Research Funding (No.2025-PUMCH-D-003).

Author Contributions

Conceptualization: Y.P., Y.S., C.S., R.L.; Methodology: Y.P., Y.S., C.S., R.L.; Formal Analysis: L.X., C.Z.; Investigation: Y.P., Y.S., C.S., R.L.; Resources: L.X., C.Z., Y.L.; Data Curation: L.X., C.Z.; Writing – Original Draft: Y.P., Y.S.; Writing – Review & Editing: Y.L.; Supervision: Y.L.; Funding Acquisition: Y.L.

Acknowledgments

We thank the trial participants and their families, investigators, and the trial staff.

Data Availability Statement

The datasets generated during and/or analyzed during the current study are not publicly available but are available from the corresponding author upon reasonable request.

Ethical Statement

This study was approved by the Ethics Committee of Peking Union Medical College Hospital (approval number: K6879). Written informed consent was obtained from all participants. For minor participants, written informed consent was obtained from their legal guardians in accordance with the Declaration of Helsinki.

Competing Interests Statement

The authors of this work have nothing to disclose.

References

1. Han, B. et al. Cancer incidence and mortality in China, 2022. J. Natl Cancer Cent. 4, 47–53. https://doi.org/10.1016/j.jncc.2024.01.006 (2024).
2. Baloch, Z. W. et al. Overview of the 2022 WHO Classification of Thyroid Neoplasms. Endocr Pathol. 33, 27–63. https://doi.org/10.1007/s12022-022-09707-3 (2022).
3. Durante, C. et al. 2023 European Thyroid Association Clinical Practice Guidelines for thyroid nodule management. Eur. Thyroid J. 12, e230067. https://doi.org/10.1530/ETJ-23-0067 (2023).
4. Ringel, M. D. et al. 2025 American Thyroid Association Management Guidelines for Adult Patients with Differentiated Thyroid Cancer. Thyroid 35, 841–985. https://doi.org/10.1177/10507256251363120 (2025).

5. Haddad, R. I. et al. NCCN Guidelines® Insights: Thyroid Carcinoma, Version 1.2025. J. Natl Compr. Canc Netw. 23, e250033. https://doi.org/10.6004/jnccn.2025.0033 (2025).
6. Sugino, K. et al. Distant Metastasis in Pediatric and Adolescent Differentiated Thyroid Cancer: Clinical Outcomes and Risk Factor Analyses. J. Clin. Endocrinol. Metab. 105, dgaa545. https://doi.org/10.1210/clinem/dgaa545 (2020).
7. Machens, A. & Dralle, H. Correlation between the number of lymph node metastases and lung metastasis in papillary thyroid cancer. J. Clin. Endocrinol. Metab. 97, 4375–4382. https://doi.org/10.1210/jc.2012-1257 (2012).
8. Li, C., Lee, K. C., Schneider, E. B. & Zeiger, M. A. *BRAF* V600E mutation and its association with clinicopathological features of papillary thyroid cancer: a meta-analysis. J. Clin. Endocrinol. Metab. 97, 4559–4570. https://doi.org/10.1210/jc.2012-2104 (2012).
9. Ma, T., Wang, L., Zhang, X. & Shi, Y. A clinical and molecular pathology prediction model for central lymph node metastasis in cN0 papillary thyroid microcarcinoma. Front. Endocrinol. (Lausanne) 14, 1075598. https://doi.org/10.3389/fendo.2023.1075598 (2023).
10. Gerlinger, M. et al. Intratumor heterogeneity and branched evolution revealed by multiregion sequencing. N. Engl. J. Med. 366, 883–892. https://doi.org/10.1056/NEJMoa1113205 (2012).
11. Zellmer, V. R. & Zhang, S. Evolving concepts of tumor heterogeneity. Cell Biosci. 4, 69. https://doi.org/10.1186/2045-3701-4-69 (2014).
12. Lv, Y. The Spatiotemporal Heterogeneity of Tumor-Associated Stromal Cells: Reprogramming Plasticity to Unlock Precision Cancer Immunotherapy. Cancer Commun. (Lond) 46, 0002. https://doi.org/10.34133/cancomm.0002 (2026).
13. Laplane, L. & Maley, C. C. The evolutionary theory of cancer: challenges and potential solutions. Nat. Rev. Cancer 24, 718–733. https://doi.org/10.1038/s41568-024-00734-2 (2024).
14. Fagin, J. A. & Nikiforov, Y. E. Progress in Thyroid Cancer Genomics: A 40-Year Journey. Thyroid 33, 1271–1286. https://doi.org/10.1089/thy.2023.0045 (2023).
15. Hernandez-Prera, J. C. & Wenig, B. M. RAS-Mutant Follicular Thyroid Tumors: A Continuous Challenge for Pathologists. Endocr Pathol. 35, 167–184. https://doi.org/10.1007/s12022-024-09812-5 (2024).
16. Sohn, S. Y. et al. Highly Concordant Key Genetic Alterations in Primary Tumors and Matched Distant Metastases in Differentiated Thyroid Cancer. Thyroid 26, 672–682. https://doi.org/10.1089/thy.2015.0527 (2016).
17. Le Pennec, S. et al. Intratumor heterogeneity and clonal evolution in an aggressive papillary thyroid cancer and matched metastases. Endocr. Relat. Cancer 22, 205–216. https://doi.org/10.1530/ERC-14-0351 (2015).
18. Masoodi, T. et al. Whole-Exome Sequencing of Matched Primary and Metastatic Papillary Thyroid Cancer. Thyroid 30, 42–56. https://doi.org/10.1089/thy.2019.0052 (2020).
19. Melo, M. et al. *TERT*, *BRAF*, and *NRAS* in Primary Thyroid Cancer and Metastatic Disease. J. Clin. Endocrinol. Metab. 102, 1898–1907. https://doi.org/10.1210/jc.2016-2784 (2017).
20. Fakhruddin, N. et al. *BRAF* and *NRAS* Mutations in Papillary Thyroid Carcinoma and Concordance in *BRAF* Mutations Between Primary and Corresponding Lymph Node Metastases. Sci. Rep. 7, 4666. https://doi.org/10.1038/s41598-017-04948-3 (2017).
21. Brumfield, A. Prevalence and Clinical Impact of *BRAF* p.V600E Mutation in Papillary Thyroid Carcinoma. Endocr Pathol. 36, 13. https://doi.org/10.1007/s12022-025-09859-y (2025).
22. Yakushina, V. D., Lerner, L. V. & Lavrov, A. V. Gene Fusions in Thyroid Cancer. Thyroid 28, 158–167. https://doi.org/10.1089/thy.2017.0318 (2018).
23. Nikiforov, Y. E. *RET*/PTC rearrangement in thyroid tumors. Endocr Pathol. 13, 3–16. https://doi.org/10.1385/ep:13:1:03 (2002).
24. Baloch, Z. W. et al. Overview of the 2022 WHO Classification of Thyroid Neoplasms. Endocr Pathol. 33, 27–63. https://doi.org/10.1007/s12022-022-09707-3 (2022).
25. Ghossein, R. A., Scholfield, D. W., Qin, H., Shaha, A. R., Ganly, I. & Xu, B. High-Grade Papillary Thyroid Carcinoma, Diffuse Sclerosing Subtype: A Series of 18 Cases Detailing the Pathologic Features, Potential for Misdiagnosis, and Aggressive Clinical Behavior. Am. J. Surg. Pathol. 49, 481–489. https://doi.org/10.1097/PAS.0000000000002371 (2025).
26. Yang, X. et al. *TERT*p Mutation Predicts Radioiodine-Refractory Character in Distant Metastatic Differentiated Thyroid Cancer. J. Nucl. Med. 58, 258–265. https://doi.org/10.2967/jnumed.116.180240 (2017).
27. Dagogo-Jack, I. & Shaw, A. T. Tumour heterogeneity and resistance to cancer therapies. Nat. Rev. Clin. Oncol. 15, 81–94. https://doi.org/10.1038/nrclinonc.2017.166 (2018).
28. Burrell, R. A., McGranahan, N., Bartek, J. & Swanton, C. The causes and consequences of genetic heterogeneity in cancer evolution. Nature 501, 338–345. https://doi.org/10.1038/nature12625 (2013).
29. Mu, Z. Z., Zhang, Y. Q., Sun, D., Lu, T. & Lin, Y. S. Effect of *BRAF* V600E and *TERT*p Mutations on Thyroglobulin Response in Patients With Distant-Metastatic Differentiated Thyroid Cancer. Endocr Pract. 28, 265–270. https://doi.org/10.1016/j.eprac.2021.12.005 (2022).
30. Moon, S. et al. Effects of Coexistent *BRAF* V600E and *TERT*p Mutations on Poor Clinical Outcomes in Papillary Thyroid Cancer: A Meta-Analysis. Thyroid 27, 651–660. https://doi.org/10.1089/thy.2016.0350 (2017).

Tables

Table 1. Clinicopathological characteristics of included patients

Characteristic	Overall cohort, N = 55[1]	Characteristic	Overall cohort, N = 55[1]
Follow-up duration (month)	27.7 (11.9, 59.3)	T stage	
Age at diagnosis (year)	31 (22, 39)	T1+T2	34 (61.8%)
Maximum diameter of PT (cm)	2.0 (1.3, 3.7)	T3+T4	21 (38.2%)
Gender		N stage	
Female	37 (67.3%)	N1a	1 (1.8%)
Male	18 (32.7%)	N1b	54 (98.2%)
recurrence risk stratification		Site of DM	
Intermediate risk	7 (12.7%)	no metastasis	11 (20.0%)
High risk	48 (87.3%)	lung only	42 (76.4%)
Number of surgeries		lung+other sites	2 (4.6%)
1 only	31 (56.4%)	Overall stage	
≥2	24 (43.6%)	I	11 (20.0%)
Pathological type		II	40 (72.7%)
PTC	53 (96.4%)	IVB	4 (7.3%)
FTC	2 (3.6%)		
1 Median (IQR); n (%)			
2 Wilcoxon rank sum exact test; Wilcoxon rank sum test; Fisher's exact test; Pearson's Chi-squared test			
Abbreviations: PT, primary tumor; DM, distant metastases			

Table 2. Concordance of genotypes between PTs and matched LNMs in overall analysis

All PT-LNM pairs (63)		Total	*BRAF* V600E mutation in PTs		Concordance rate	Kappa coefficient
			Wild type	mutation		
BRAF V600E mutation in LNMs	Wild type	39	34	5	92.1%(58/63)	0.84
	mutation	24	0	24		
		Total	*TERT*p mutation in PTs		Concordance rate	Kappa coefficient
			Wild type	mutation		
*TERT*p mutation in LNMs	Wild type	60	60	0	98.4%(62/63)	0.79
	mutation	3	1	2		
		Total	*NTRK3* fusion in PTs		Concordance rate	Kappa coefficient
			Wild type	mutation		
NTRK3 fusion in LNMs	Wild type	61	60	1	98.4%(62/63)	0.79
	mutation	2	0	2		
		Total	*RET* fusion in PTs		Concordance rate	Kappa coefficient
			Wild type	mutation		
RET fusion in LNMs	Wild type	44	44	0	100.0%(63/63)	1.00
	mutation	19	0	19		

Abbreviations: PT, primary tumor; LNM, lymph node metastasis; PT-LNM pairs, primary tumor-lymph node metastasis pairs; *TERT*p, *TERT* promoter

Table 3. Concordance of genotypes between PTs and matched LNMs in the synchronous group

synchronous group (41)		Total	*BRAF* V600E Mutation in PTs		Concordance rate	Kappa coefficient
			Wild type	Mutation		
BRAF V600E mutation in LNMs	Wild type	29	25	4	90.2%(37/41)	0.79
	Mutation	12	0	12		
		Total	*TERT*p Mutation in PTs		Concordance rate	Kappa coefficient
			Wild type	Mutation		
*TERT*p mutation in LNMs	Wild type	0	41	0	100.0%(41/41)	1
	Mutation	0	0	0		
		Total	*NTRK3* fusion in PTs		Concordance rate	Kappa coefficient
			Wild type	Mutation		
NTRK3 fusion in LNMs	Wild type	40	39	1	97.6%(40/41)	0.66
	Mutation	1	0	1		
		Total	*RET* fusion in PTs		Concordance rate	Kappa coefficient
			Wild type	Mutation		
RET fusion in LNMs	Wild type	27	27	0	100.0%(41/41)	1
	Mutation	14	0	14		

Abbreviations: PT, primary tumor; LNM, lymph node metastasis; *TERT*p, *TERT* promoter

Table 4. Concordance of genotypes between PTs and matched LNMs in the asynchronous group

asynchronous group (22)		Total	*BRAF* V600E Mutation in PTs		Concordance rate	Kappa coefficient
			Wild type	Mutation		
BRAF V600E mutation in LNMs	Wild type	10	9	1	95.5%(21/22)	0.91
	Mutation	12	0	12		
		Total	*TERT*p Mutation in PTs		Concordance rate	Kappa coefficient
			Wild type	Mutation		
*TERT*p mutation in LNMs	Wild type	19	19	0	95.5%(21/22)	0.78
	Mutation	3	1	2		
		Total	*NTRK3* fusion in PTs		Concordance rate	Kappa coefficient
			Wild type	Mutation		
NTRK3 fusion in LNMs	Wild type	21	21	0	100.0%(22/22)	1
	Mutation	1	0	1		
		Total	*RET* fusion in PTs		Concordance rate	Kappa coefficient
			Wild type	Mutation		
RET fusion in LNMs	Wild type	17	17	0	100.0%(22/22)	1
	Mutation	5	0	5		

Abbreviations: PT, primary tumor; LNM, lymph node metastasis; *TERT*p, *TERT* promoter

Table 5. Comparison of genotypes between PTs and matched LNMs in overall analysis

	PTs (63)[1]	LNMs (63)[1]	p-value[2]
BRAF V600E mutation			0.367
Mutation	29 (46.0%)	24 (38.1%)	
wild type	34 (54.0%)	39 (61.9%)	
*TERT*p mutation			>0.999
Mutation	2 (3.2%)	3 (4.8%)	
wild type	61 (96.8%)	60 (95.2%)	
NTRK3 fusion			>0.999
Mutation	3 (4.8%)	2 (3.2%)	
wild type	60 (95.2%)	61 (96.8%)	
RET fusion			>0.999
Mutation	19 (30.2%)	19 (30.2%)	
wild type	44 (69.8%)	44 (69.8%)	

1 n (%)

2 Pearson's Chi-squared test; Fisher's exact test

Abbreviation: PT, primary tumor; LNM, lymph node metastasis; *TERT*p, *TERT* promoter

Figures

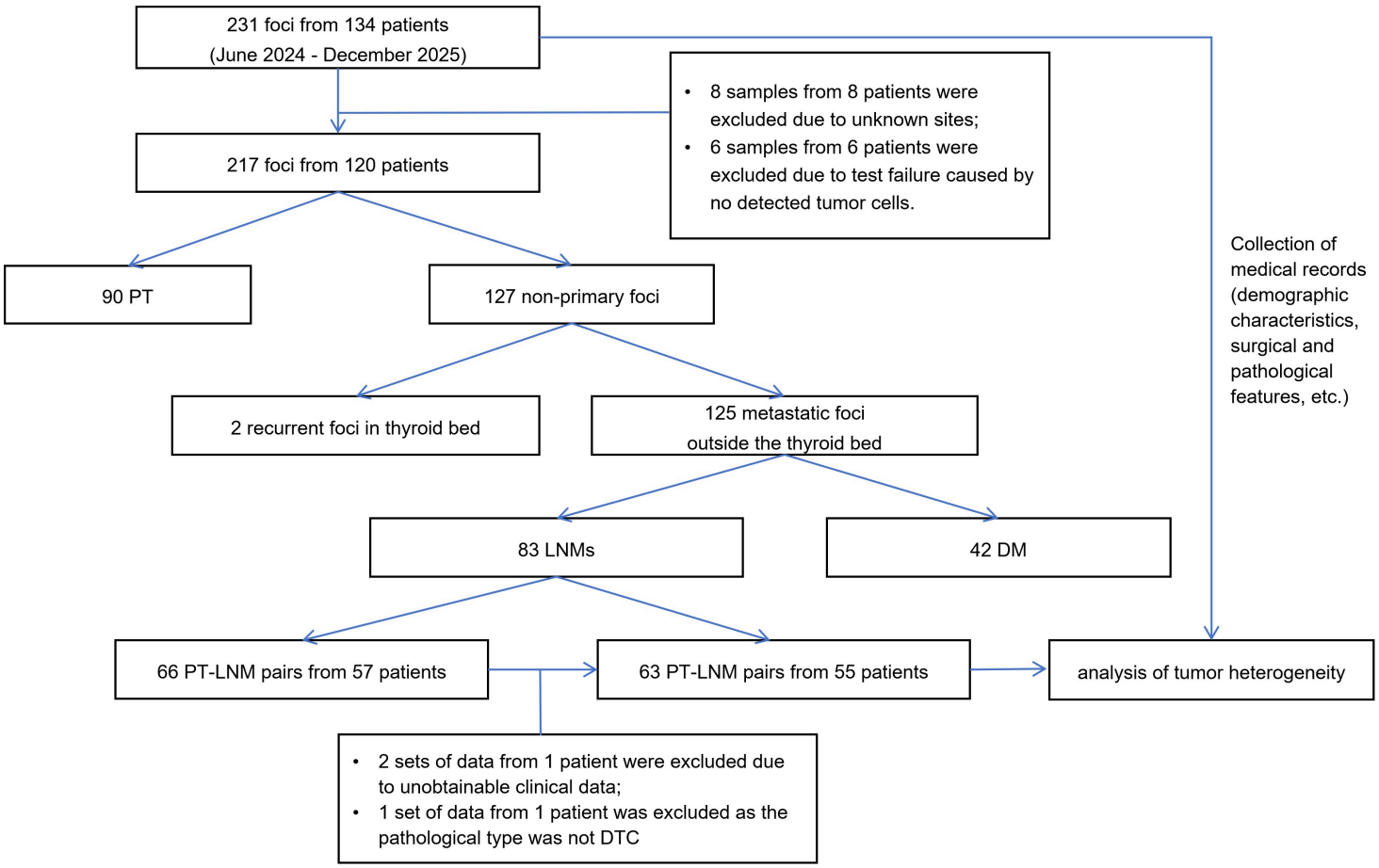


Figure 1

Flow chart, including part of the screening process.(After screening, a total of 63 PT-LNM pairs from 55 patients were included in the final analysis)

Abbreviation: PT, primary tumor; LNM, lymph node metastasis; DM, distant metastasis; PT-LNM pairs, primary tumor-lymph node metastasis pairs

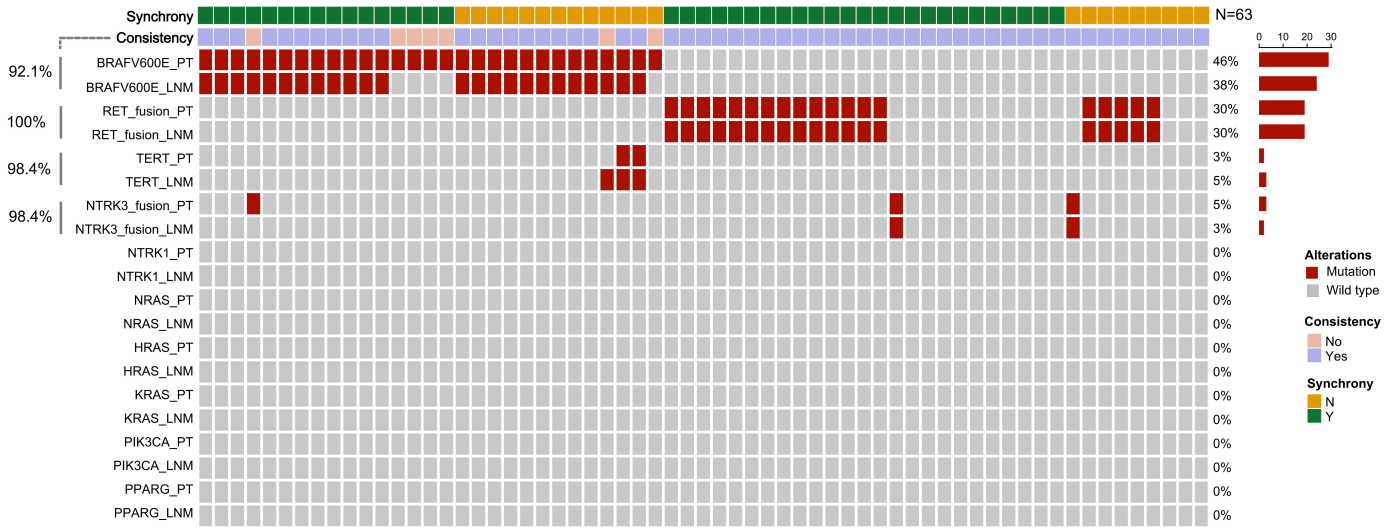


Figure 2

Mutational landscape of overall cohort. (Synchrony indicates whether PT and LNM are synchronous, with green for synchronous and yellow for asynchronous. Concordance indicates whether PT and LNM genetic testing results are consistent, with purple for consistent and pink for inconsistent. Alterations indicate presence of genetic alterations, with red for presence and gray for absence.)

Abbreviation: PT, primary tumor; LNM, lymph node metastasis; N, no; Y, yes

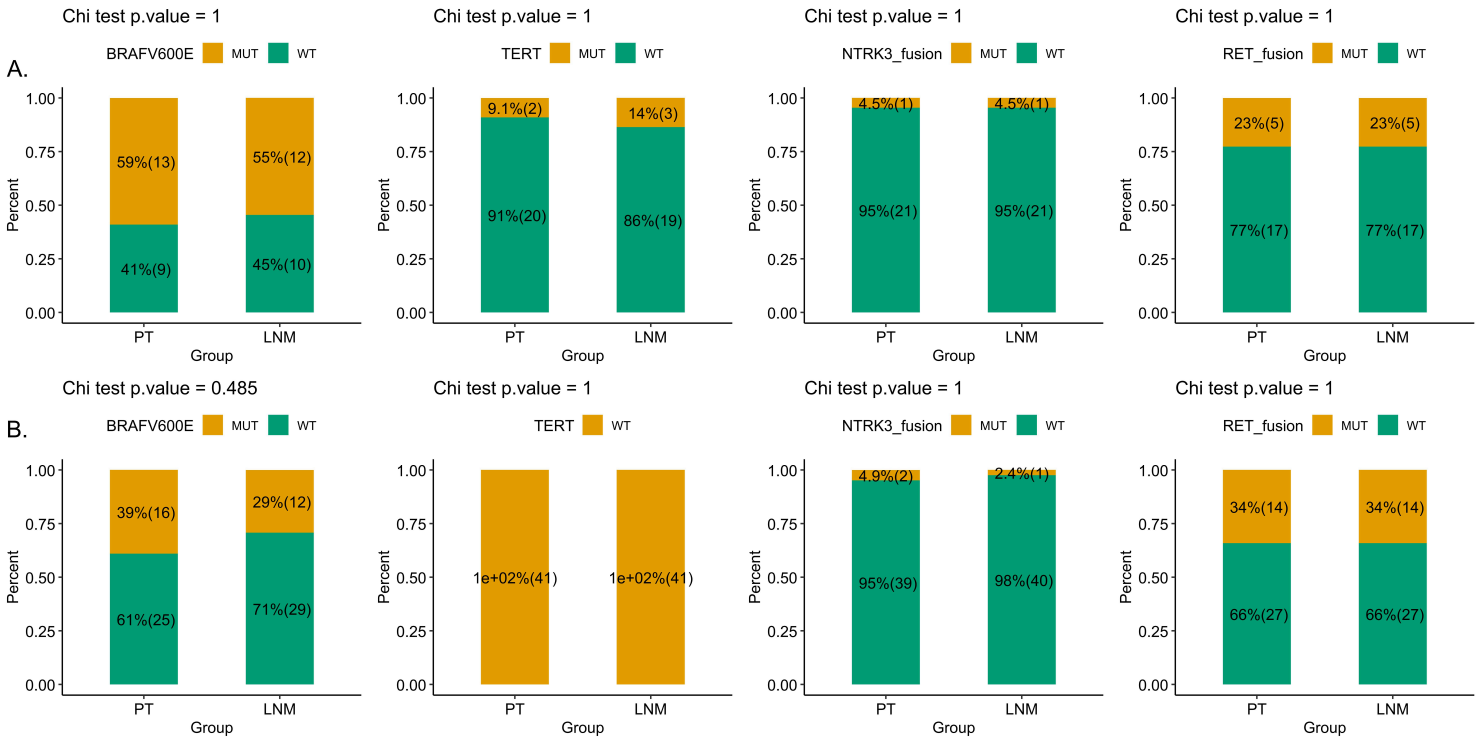


Figure 3

Comparison of genotypes between PTs and LNMs in subgroups. (A) Comparison of genotypes between PT and LNM in the synchronous group; (B) Comparison of genotypes between PT and LNM in the asynchronous group. (Yellow indicates the number and proportion of patients with the detected mutation. Green indicates the number and proportion of patients with wild-type genotype)

Abbreviation: PT, primary tumor; LNM, lymph node metastasis; MUT, mutation; WT, wild type